New Journal of Physics
An Institute of Physics and Deutsche Physikalische Gesellschaft Journal

Direct measurement and analysis of the carrier-envelope phase in light pulses approaching the single-cycle regime

P Dombi[1,7], A Apolonski[1,2], Ch Lemell[3], G G Paulus[4], M Kakehata[5], R Holzwarth[6], Th Udem[6], K Torizuka[5], J Burgdörfer[3], T W Hänsch[6] and F Krausz[1,6]

[1] Institut für Photonik, Technische Universität Wien, Gusshausstr. 27, A-1040 Wien, Austria
[2] Institute of Automation and Electrometry, SB RAS, Novosibirsk 630090, Russia
[3] Institut für Theoretische Physik, Technische Universität Wien, Wiedner Hauptstrasse 8, A-1040 Wien, Austria
[4] Texas A&M University, Physics Department, College Station, TX 77843-4242, USA
[5] National Institute of Advanced Industrial Science and Technology (AIST), 1-1-1 Umezono, Tsukuba 305-8568, Japan
[6] Max-Planck-Institut für Quantenoptik, Hans-Kopfermann-Str. 1, D-85748 Garching, Germany
E-mail: dombi@tuwien.ac.at

New Journal of Physics **6** (2004) 39
Received 15 January 2004
Published 29 March 2004
Online at http://www.njp.org/ (DOI: 10.1088/1367-2630/6/1/039)

Abstract. We demonstrate a solid-state device capable of providing direct information about the carrier-envelope (CE) phase of ultrashort (4 fs) laser pulses. The measurement is based on multi-photon-induced photoelectron emission from a gold surface. The amount of the charge emitted from the surface gives a clear indication of phase sensitivity, as predicted by our simulations and also by a simple intuitive model. This phenomenon was used to determine the CE phase value of each laser pulse in a mode-locked, unamplified, low-energy pulse train. The inability of the commonly used f-to-$2f$ interferometric method to measure accurately extracavity drifts of the CE phase is discussed and contrasted with the direct phase measurement method proposed here. The evolution of the CE phase upon propagation of pulses comparable in duration to the optical cycle is analysed.

[7] Author to whom any correspondence should be addressed.

PII: S1367-2630(04)74660-1

Contents

1. Introduction

The carrier-envelope (CE) phase of mode-locked laser pulses [1] (sometimes also referred to as the 'absolute' phase) accounts for the timing of the oscillations of the electric field with respect to the intensity envelope of the pulse (see figure 1). It has become increasingly important for ever shorter pulses in recent years. Strong-field atomic processes driven by few-cycle pulses were found to exhibit sensitivity to the CE phase [2]. The importance of the CE phase in intense field–matter interactions and possible ways of measuring its value were initially analysed theoretically [3]–[12]. Recently, it has been confirmed experimentally that both above-threshold ionization [13, 14] and high-harmonic generation [15] depend sensitively on the CE phase. This dependence can be used to determine its value for each laser pulse. However, measurement techniques relying on these and related strong-field processes have the inherent drawback that they require high-energy ($\gg 1\ \mu$J), amplified laser pulses, a complex vacuum system and sophisticated detectors.

At the front end of laser systems used to investigate femto- and attosecond physics, one finds a mode-locked laser oscillator delivering a train of pulses where the CE phase changes continuously from one pulse to the other (see figure 1) owing to the difference between the group and phase velocities of the pulse circulating in the laser cavity. In conventional mode-locking, this CE phase shift jitters mainly due to pulse energy fluctuations and optical non-linearities in the cavity [1]. Using the so-called f-to-2f interferometry or self-referencing technique [16]–[18], this pulse-to-pulse shift can be stabilized and locked to an arbitrary frequency [19]–[23]. CE phase stabilization has revolutionized optical frequency metrology [24] and made experimental investigations of extreme non-linear optical processes with phase-stabilized pulses possible [15]. However, an f-to-2f interferometer, as opposed to the above-mentioned extreme non-linear optical processes, is not capable of reliably measuring the actual ('absolute') value of the CE phase; it is suitable for accessing (and thus controlling) its pulse-to-pulse shift only.

A recent proposal suggested that a possible way of circumventing current limitations and providing direct access to the CE phase in low-energy pulses is to make use of the sensitivity of multi-photon-induced photoelectron emission from a metal surface to the CE phase [25]. The emitted charge from the surface was found to exhibit a robust phase dependence for pulses comprising merely a few wave cycles and impinging on the surface at grazing incidence with their electric field vector lying in a plane perpendicular to the surface ('P' polarization). Most importantly, the intensity requirements were predicted to be greatly relaxed when compared with recent strong-field experiments [13]–[15].

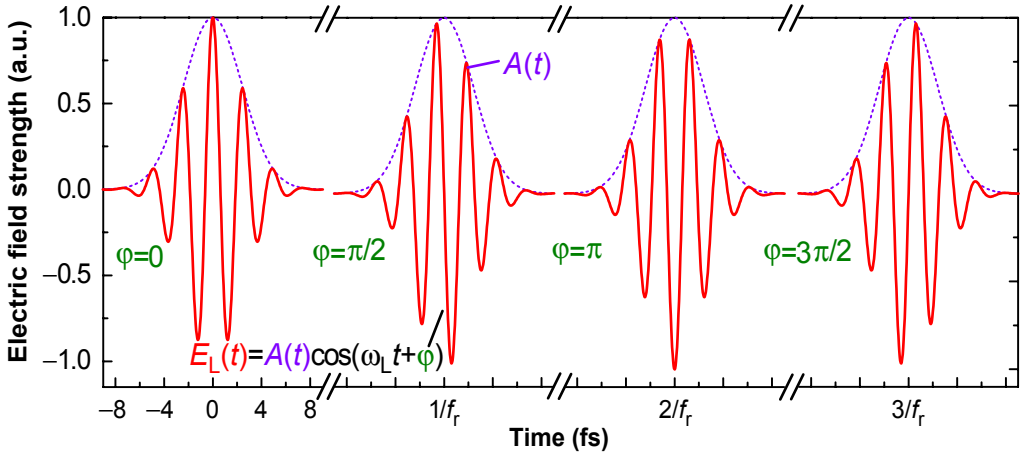

Figure 1. Evolution of the electric field $E_L(t)$ of few-cycle laser pulses (τ_L = 4 fs, λ_0 = 750 nm, Gaussian pulse shape: $A(t) = A_0 \exp(-2t^2 \ln 2/\tau_L^2)$, repetition rate: f_r) with φ slipping by $\Delta\varphi = 2k\pi + \pi/2$ (k is an unknown integer) upon each round-trip in the mode-locked laser, i.e. from one pulse to the next in the pulse train emitted by the laser oscillator.

In this paper, we further examine the pulse length and pulse shape dependence of phase-sensitive photoelectron emission by numerical simulation. A simple intuitive model also backs major conclusions. Then we present experimental evidence of the predicted CE phase sensitivity of multi-photon-induced photoelectron emission using 4 fs pulses with an energy of only 3 nJ. It is described how this phenomenon can be utilized to determine the CE phase evolution in a multi-MHz pulse train. Finally, we contrast the photoemission-based phase measurement with the f-to-2f technique and conclude that the latter fails to track accurately (and compensate for) extracavity CE phase shifts.

2. Simulation results

We use the CE description for the temporal electric field evolution of a laser pulse. The electric field can be unambiguously decomposed into a carrier wave and an envelope in the form of $E_L(t) = A_L(t)\cos(\omega_L t + \varphi)$, if one fixes ω_L as the centre of gravity of the spectral intensity distribution of the pulse. This procedure yields a reasonably smooth envelope, $A_L(t)$, in almost all practical cases. For a self-consistent description, it is also necessary that the full-width at half-intensity maximum (FWHM) pulse length, τ_p, is longer than the oscillation period of the carrier wave [2]. Satisfaction of this condition ensures that ω_L and $A_L(t)$ remain invariant to a change of φ, which is necessary for examining any phase-sensitive phenomenon. The $\tau_p > 2\pi/\omega_L$ condition is met even for the shortest visible laser pulses available to date [26]–[28], permitting an unambiguous and consistent definition of φ.

In general, φ tends to evolve on significantly shorter propagation lengths than the pulse shape. For example, for a 4-fs-long Gaussian pulse centred at 750 nm, the characteristic propagation length of CE phase evolution is about 25 μm in fused silica, on which a pulse with φ=0 changes into a pulse with $\varphi = \pi$. Such a small amount of dispersion does not change significantly the

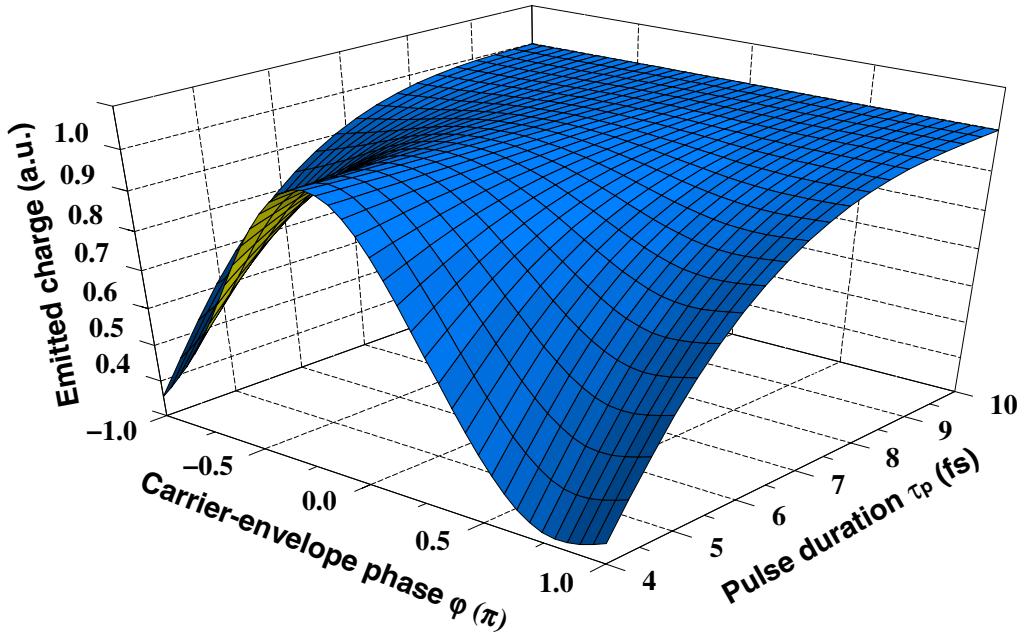

Figure 2. Computed charge emitted from a gold surface (modelled as a confined free-electron gas (jellium); see [25] for further details) exposed to a Gaussian laser pulse ($\lambda_0 = 750\,\mathrm{nm}$, $I_\mathrm{p} = 5 \times 10^{12}\,\mathrm{W\,cm^{-2}}$) at grazing incidence as a function of the CE phase φ. Pulse durations range from 4 to 10 fs. The light is incident with the electric field oriented along the surface normal ('P' polarization). The carrier-envelope phase is defined by $E_\mathrm{L}(t) = A_\mathrm{L}(t)\cos(\omega_\mathrm{L}t + \varphi)$ with $E_\mathrm{L}(t) > 0$ implying a field directed into the irradiated matter.

pulse shape even for such a short pulse. However, for ultrabroad-band pulses with τ_p approaching $T_0 = 2\pi/\omega_\mathrm{L}$, a variation of φ may not be completely decoupled from that of $A(t)$. Implications of this will be scrutinized in section 5.

Previous simulations based on time-dependent density functional theory [25] predicted that the photoelectron yield of emission from a metal surface (modelled as a confined free-electron gas using the jellium model) exhibits a robust dependence on φ in a parameter range broad enough for practical use. However, several conditions have to be met. The first and most intuitively justifiable one is that the pulse must be short enough to contain just a few oscillation cycles. Pulses significantly shorter than 10 fs are required at $\lambda_\mathrm{L} = 750\,\mathrm{nm}$, where $T_0 = 2.5\,\mathrm{fs}$, to induce a substantial variation of the photocurrent with φ, as shown in figure 2. In the simulation geometry, the laser pulse impinged on the surface at grazing incidence and polarization 'P' with an on-axis peak electric field of $E_\perp \approx 6 \times 10^7\,\mathrm{V\,cm^{-1}}$, corresponding to a peak intensity of $5 \times 10^{12}\,\mathrm{W\,cm^{-2}}$. The material chosen was gold with a work function of approximately 5 eV, implying that simultaneous absorption of at least three photons with a typical laser wavelength of 750 nm is needed for emission to take place. For a 10 fs, 750 nm pulse, there is hardly any observable difference between the electron yield of a '*cosine*' pulse ($\varphi = 0$) and a '*minus cosine*' pulse ($\varphi = \pi$), whereas at $\tau_\mathrm{p} = 4\,\mathrm{fs}$, a drastic phase effect is seen. Similar conclusions were recently drawn from phenomenological considerations [29].

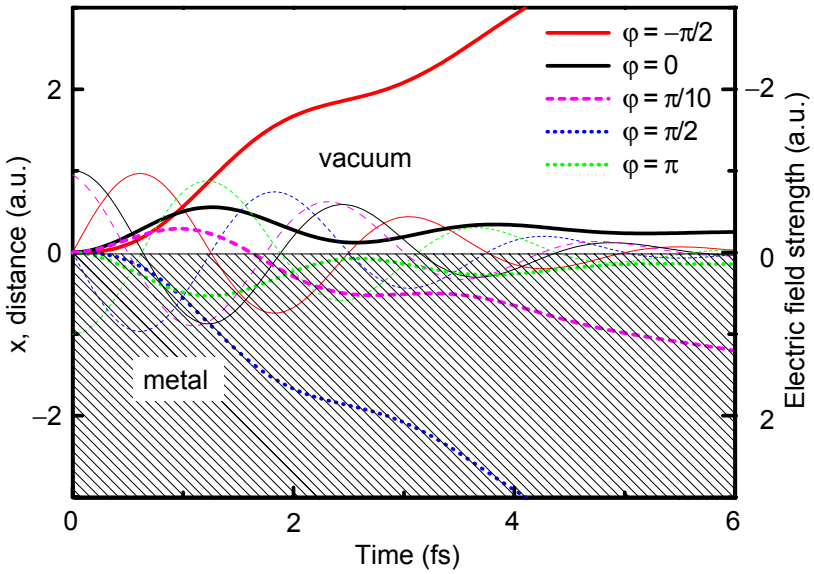

Figure 3. Classically computed trajectories (thick lines) of the emitted photoelectrons in vacuum above the surface of the cathode (positioned at $x = 0$) upon interaction with the field of the laser pulse (thin lines, note the reverse axis) for different CE phases. The electron is assumed to be emitted at the peak of the laser pulse envelope ($t = 0$). Outside the favoured range of $-\pi/2 \leqslant \varphi < 0$ (black and red curves), the electrons will be pushed back on to the surface by the electric field of the laser pulse either right after their bound-free transition (green and blue curves) or after performing a wiggle in the laser field (magenta curve).

Our simulations have also revealed that the emitted charge per pulse has a maximum at a phase value of $\varphi_{\max} = -\pi/4$ (see figure 2), implying maximum strength of the electric field (pulling the electrons away from the surface) some 300 as after the pulse peak, and that it is invariant to the temporal structure and peak intensity of the pulse shape in the regime of multi-photon ionization. The prediction for the location of the maximum can be explained in the framework of a simple model using the fact that the light intensity is in a range typical of the perturbative regime of multi-photon absorption. Therefore, electrons are emitted with low kinetic energy ($<\hbar\omega_{\mathrm{L}}$) within a narrow time interval strictly centred at the peak of the pulse envelope. After that, in a first approximation, these electrons are steered in the vacuum by the laser field, which is much stronger than the static electric field applied to extract and observe the photoelectrons than the mirror-charge field.

On the basis of this picture, several electron trajectories were determined classically and it was found that for carrier-envelope phases in the range of $-\pi/2 \leqslant \varphi < 0$, the electrons undergoing bound–free transition at the peak of the pulse envelope are initially pulled away from the surface and never return during the pulse (see thick solid red and black curves in figure 3). If the CE phase value is outside this distinguished 'escape range', there are two different possibilities. The first is that at the time of birth of the electrons (at the pulse peak) the instant field points away from the surface and immediately pushes back the electrons into the metal (thick dotted blue and green curves in figure 3). Recapturing of the electrons by the metal can also happen somewhat later, after they perform a wiggle in the laser field (thick

dashed magenta curve in figure 3). It is a unique feature of few-cycle laser pulses that multi-photon-induced bound–free transitions are distributed over a period shorter than the optical cycle at the peak of the pulse envelope. This results in increased sensitivity of the centre-of-gravity motion of the electron cloud to the CE phase and in maximum electron extraction efficiency near the centre of the above determined 'escape range', i.e. at around $\varphi_{\max} = -\pi/4$. From these arguments, it is also obvious that for longer pulses the broad temporal distribution of bound–free transitions along the pulse blurs the phase sensitivity of multi-photon-induced photoelectron emission.

In our studies, following [25], the phase sensitivity was checked for the most commonly used analytic intensity profiles, for some specific pulses with satellites and for some typical intensity profiles delivered by our laser system [26], but in all of these cases we found the same quantitative behaviour with merely the modulation depth (i.e. the extent of the sensitivity of the total emitted charge to the CE phase) being subject to a slight pulse shape dependence. From this analysis, we derive $\varphi_{\max} = -\pi/4 \pm \pi/10$, with the uncertainty originating from limitations of numerical accuracy.

Another important requirement for a pronounced and robust phase effect is the dominance of multi-photon processes in photoelectron production [25]. Even though some sensitivity to the CE phase prevails at higher intensities, in the tunnelling regime, the phase calibration will be different, i.e. the position of the maximum of the signal, $\varphi_{\max}$, in figure 2 will be located at a different carrier-envelope phase value [25]. The reduction of phase sensitivity at higher intensities seems somewhat surprising at first glance since, taking into account the adiabatic nature of tunnelling emission as opposed to the multi-photon regime (which is clearly seen in figure 2 of Lemell *et al* [25]), one would expect a less pronounced phase effect in the latter. The simple picture described above, however, can explain the strong phase effect expected in that case as well.

3. Phase diagnostics on the short-pulse laser system

For experimental verification of these predictions, we developed a laser system delivering 4 fs, 3 nJ pulses at a central wavelength of 700–750 nm and a repetition rate of $f_r = 24$ MHz (figure 4, dashed box) [26]. The pulse-to-pulse shift of the CE phase, $\Delta\varphi$, was actively stabilized with an f-to-$2f$ interferometer using only 15% of the laser output. The split-off beam was sent into a photonic crystal fibre to broaden the laser spectrum beyond one octave to allow beating of the second harmonic of the red wing of the spectrum with the blue wing of the fundamental. This beating signal at a frequency of $f_{ceo} = (\Delta\varphi/2\pi) f_r$, exactly gives the reproduction frequency of φ in the laser pulse train and it is also called the carrier-envelope offset frequency, since in the frequency domain picture of the pulse train it gives the offset of the frequency comb from zero frequency. After having generated this signal at f_{ceo} in an f-to-$2f$ interferometer, we fed it into the phase stabilization servo loop, the output of which is used to modulate the power of the pumping beam of the laser oscillator through an electro-optical modulator. Feedback is achieved by utilizing the fact that $\Delta\varphi$ and thus f_{ceo} depend on the pump power due to Kerr non-linearities in the laser crystal. Changes in the non-linear refractive index result in a modified difference between the intracavity group and phase velocities for the circulating pulse and, making use of this effect, one can actively lock f_{ceo} in the output pulse train either to an external reference signal provided by a rf frequency synthesizer (at $f_{ref} = 1$ MHz in our case; electronic connections shown by

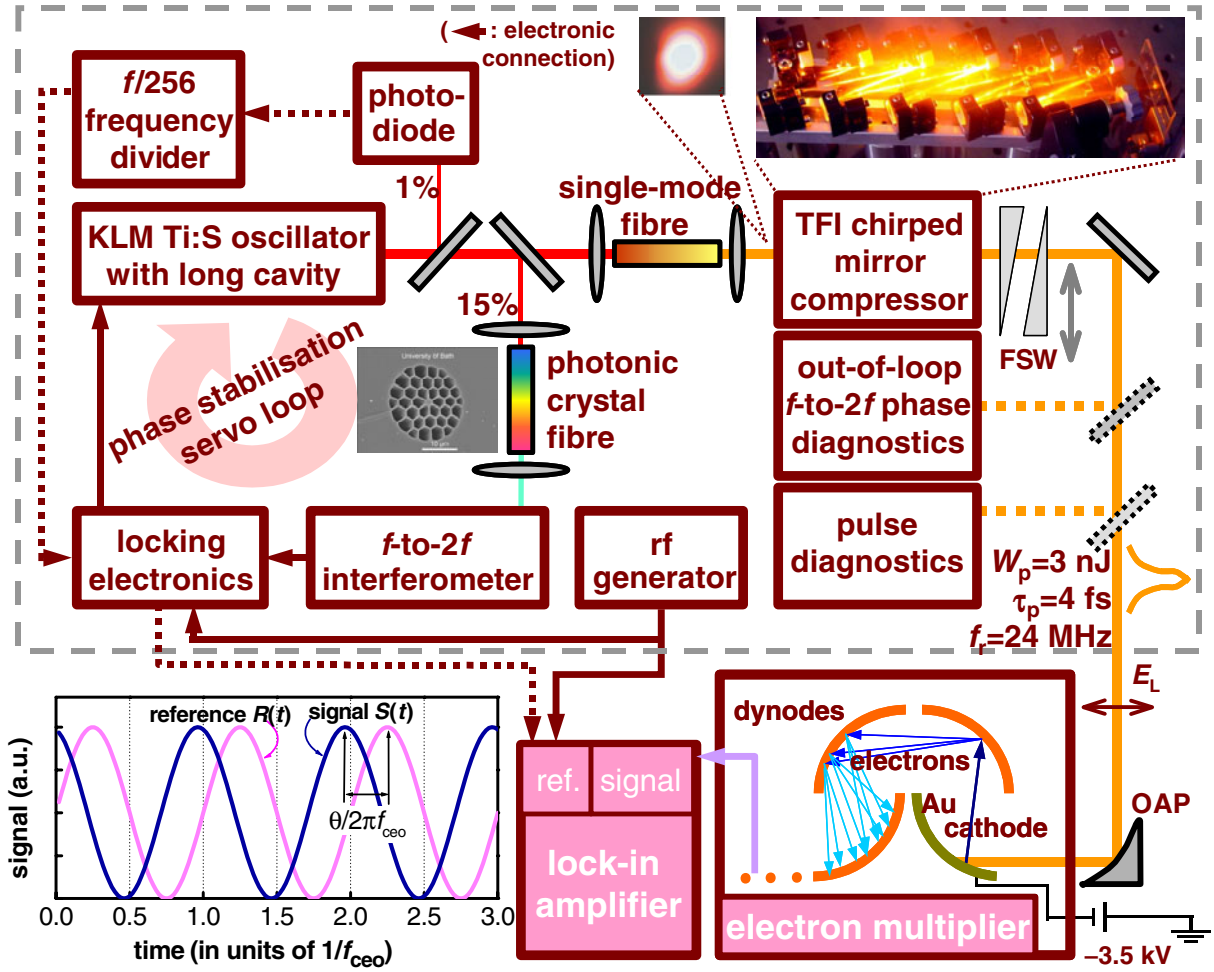

Figure 4. Schematic representation of the experiment. The long-cavity ($f_r \approx$ 24 MHz) Kerr-lens-mode-locked Ti:sapphire laser is carrier-envelope-phase-locked with the f-to-$2f$ self-referencing technique and supplemented with a pulse compressor delivering 4 fs, 3 nJ pulses. The laser consists of a thin highly-doped Ti:sapphire crystal and dispersive chirped multi-layer mirrors and produces 10 fs pulses. The cavity incorporates an imaging all-reflective delay line for reducing the pulse repetition frequency. The extracavity pulse compression stage is made up of a 1.5-mm-long conventional fused-silica single-mode fibre and a few special chirped mirrors introducing tailored group-delay dispersion over the wavelength range of 500–1000 nm [30]. The carrier wavelength of the pulses emerging from the fibre is between 700 and 750 nm, depending on the actual fibre length and input pulse energy. The unknown carrier-envelope phase of the phase-controlled pulse train generated is shifted by precisely known amounts by translation of one of a pair of thin fused-silica wedges (FSW). It is subsequently measured by focusing the 4-fs, 'P'-polarized beam with an off-axis parabola (OAP) onto a gold photocathode and detecting the phase shift θ of the amplified multi-photon-induced photoemission signal $S(t)$ from the gold with respect to a reference signal $R(t)$ to which the evolution of $\varphi = \varphi_0 + 2\pi f_{\mathrm{ref}} t$ is phase-locked.

solid lines in figure 4) or, alternatively, to a signal derived by digital frequency division from the pulse repetition frequency ($f_{\mathrm{ref}} = f_{\mathrm{r}}/n \approx 93\,\mathrm{kHz}$, in our case with $n = 256$; dotted electronic connections in figure 4). This latter option has the advantage that exactly every nth pulse has the same (but by this method still undetectable) CE phase.

The rest of the output of the laser is externally broadened in a 1.5-mm-long, conventional, single-mode, fused silica fibre and subsequently compressed in a tilted-front-interface chirped-mirror compressor [30] to a duration of $\tau_{\mathrm{p}} = 4\,\mathrm{fs}$ [26]. With the phase-locking loop in operation, the phase slips by $\Delta\varphi = 2\pi(f_{\mathrm{ref}}/f_{\mathrm{r}})$ from pulse to pulse. First, we tested the f-to-$2f$ phase-locking loop with a second, independent, out-of-loop f-to-$2f$ beat signal detector. To this end, we focused the 4-fs pulses carried at $\lambda_0 \approx 710\,\mathrm{nm}$ into a 0.1-mm-thick ZnO crystal. For optimized second-harmonic generation of the infrared part of the broadband radiation, the polished surface of the ZnO crystal has a crystallographic orientation of (1120). The second harmonic of the low-frequency spectral components near $\lambda_{\mathrm{l}} = 1000\,\mathrm{nm}$ beat with the high-frequency components around $\lambda_{\mathrm{h}} = \lambda_{\mathrm{l}}/2 = 500\,\mathrm{nm}$ (as in [10]), resulting in an f-to-$2f$ signal at 500 nm modulated at f_{ceo} ($=f_{\mathrm{ref}}$ with the servo loop in operation). Careful spectral filtering allows this signal to be detected with a photodiode and with an electronic spectrum analyser. The beat signal is typically 30 dB above noise in a resolution bandwidth of 10 kHz.

The beat component $S(t)$ of the signal of the f-to-$2f$ interferometer oscillates with a frequency f_{ceo} and can be written as $S(t) = S_0\cos(2\pi f_{\mathrm{ceo}}t + \theta)$. This signal is phase-locked to an external reference, $R(t) = R_0\cos(2\pi f_{\mathrm{ref}}t)$, yielding $f_{\mathrm{ceo}} = f_{\mathrm{ref}}$. As a consequence, phase-sensitive, narrow-band (lock-in) amplification is ideally suited to detect $S(t)$. The lock-in amplifier is able to measure directly both the amplitude S_0 and the phase θ or, alternatively, it can acquire the in-phase ($X = S_0\cos\theta$) and the quadrature ($Y = S_0\sin\theta$) components of the input signal. This latter pair of output parameters provides, of course, the same, full information on the signal to be measured as the S_0, θ parameter pair. Whilst this out-of-loop f-to-$2f$ measurement allows the jitter of φ to be determined, it is not suitable for measuring it, as will be revealed in section 5.

To confirm that the observed signal indeed originates from the evolution of φ in the laser pulse train, we introduced a path of variable length through a pair of thin fused silica wedges (FSW in figure 4) and measured the variation of the in-phase component of the lock-in output, $X = S_0\cos\theta$, as a function of the change ΔL in the fused silica path length. The result is shown in figure 5. The sinusoidal oscillation in X is accounted for by the fact that θ varies linearly with the path length $\theta = \theta_0 + \pi(\Delta L/L_{f\text{-to-}2f})$, with the period length being evaluated as $L_{f\text{-to-}2f} = 20.9 \pm 0.7\,\mu\mathrm{m}$ from a least-squares fit (line in figure 5) to the measured data (triangles), the details of which will be discussed below. This is in excellent agreement with the theoretical value of $L_{f\text{-to-}2f} = 21.5\,\mu\mathrm{m}$ (see section 5).

Tracking the out-of-loop f-to-$2f$ signal in the time domain at a fixed value of ΔL over a period of 10 min yielded an rms CE-phase jitter of less than 1.2 rad, indicating good long-term control of θ (and thereby φ) in the 4-fs pulse train. In similar laser systems, more detailed out-of-loop studies of this effect were conducted [31, 32], partly also by resolving phase noise spectrally. These experiments yielded less phase jitter over similar acquisition times. However, in both of the referred studies, two identical f-to-$2f$ interferometers were used: one in the stabilization loop and one for measurement. This gives rise to some cancellation of real noise of the CE phase because of common mode rejection by similar amplitude-to-phase coupling mechanisms [33, 34] in both interferometers. In our system, the octave spanning light signal for the stabilization f-to-$2f$ interferometer is generated in a photonic crystal fibre completely different from the conventional fibre in which the major portion of the beam is propagated. This

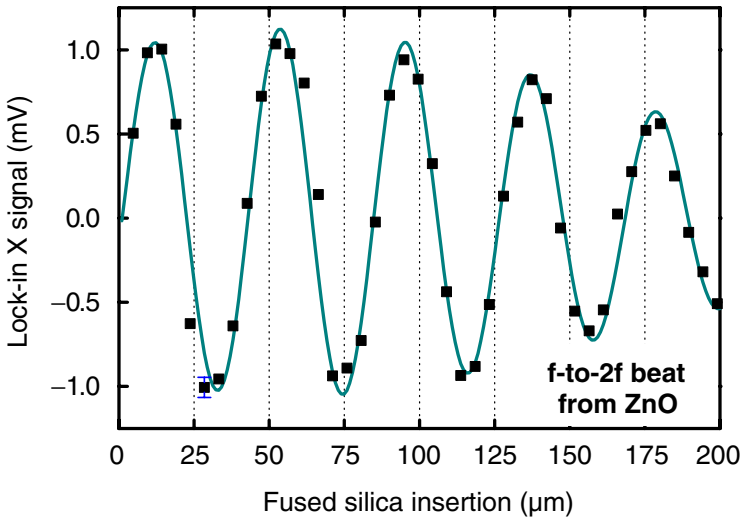

Figure 5. In-phase, $X = S_0 \cos\theta$ component of the lock-in amplifier output as a function of the change in path length through the fused silica glass wedges. The lock-in input signal is the f-to-$2f$ beat note from a ZnO crystal. The fit to the measurement data points was made on the assumption of an amplitude dependence of the signal as $S_0 \sim I_p^x$ with $x = 2$. The peak intensity drops owing to dispersive pulse broadening upon propagation in the wedge material.

results in higher sensitivity for the noise of the CE phase when compared with the noise of the measurement system; therefore, we overestimate the real CE phase noise at the output.

4. Phase-sensitive photoelectron emission from a gold surface

Having been successfully tested by the out-of-loop f-to-$2f$ phase diagnostic system, our measurement apparatus can be used for studying the CE phase dependence of multi-photon-induced photoemission from a metal surface. For the generation and low-noise pre-amplification of the photocurrent, we used a commercial electron multiplier tube (EMT) equipped with a gold photocathode (R595, Hamamatsu), kept under 10^{-5} mbar. The laser beam was focused on to the cathode with an off-axis parabola with an f-number of 2 at an angle as close to grazing incidence as allowed by the vacuum chamber geometry ($\approx 70^\circ$). With a spot diameter of 7 μm, the on-target peak intensity was $I_p \approx 2 \times 10^{12}$ W cm^{-2}, corresponding to a peak electric field strength normal to the surface of $E_\perp \approx 4 \times 10^7$ V cm^{-1}. In the 10^{12}–10^{13} W cm^{-2} peak intensity range, the time-averaged output current from the electron multiplier tube (having a typical gain of 4×10^7), measured with an electronic spectrum analyser, was found to follow a power-law scaling, $\propto I_p^x$ (figure 6), indicating multi-photon-induced transitions [25, 35]. The evaluated value of x between 3.2 and 3.7 can be reconciled with the approximately 5-eV work function of gold and the spectral intensity distribution of the laser pulses. From the measured value of the output current we could also conclude that the number of the emitted electrons from the cathode was less than one per laser shot.

As a further preliminary test, we measured the dependence of the non-linear photoemission signal on shifting of one of the fused silica wedges at the output of the pulse compressor (FSW

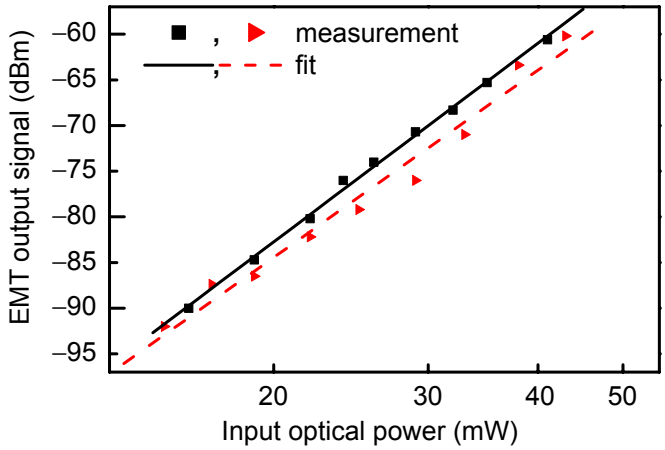

Figure 6. Intensity dependence of the output signal of the electron multiplier tube (EMT). x-axis: average power delivered by the pulse train measured before the TFI chirped mirror compressor, logarithmic scale; y-axis: output signal of the EMT (also logarithmic scale) at the pulse repetition rate measured by an electronic spectrum analyser. The power-law scaling of the photoemission signal is a characteristic of the multi-photon regime, as also seen in figure 1 of Lemell *et al* [25]. The linear fit to the measured data points resulted in slopes of 3.6 ± 0.1 and 3.4 ± 0.2, respectively.

in figure 4). The amplitude of the output signal from the multiplier tube, S_0, measured with the lock-in amplifier referenced to the repetition rate of our laser, f_r, exhibits a rapid decay with ΔL as a consequence of dispersive effects. Although the pulses broaden only by a few per cent upon travelling a distance of a few tens of micrometres in fused silica, the resultant decrease in their peak intensity is sufficient to lower the photocurrent appreciably, owing to the higher-order I_p^x scaling discussed above (figure 7, black triangles). An excellent fit to these measurement points can be achieved by taking the retrieved temporal pulse (envelope) shape from our pulse diagnostic system [26] and simulating its linear, dispersive propagation in the wedge material (fused silica). The computed value of the peak intensity at each wedge position can then be raised to the power of x to fit the curve. Optimization yielded $x = 3$, resulting in the black solid fit in figure 7. Indeed, the photoemission is expected to be a third-order process for most of the photons of the laser pulse, and this method also corroborates previous pulse diagnostic results [26] since a very unrealistic pulse shape would make the best-fit x value differ much more from the independently measured one (see figure 6).

After these diagnostic and preparatory measurements we focused on checking the phase sensitivity of photoelectron emission. As φ evolves with a constant rate in the phase-controlled pulse train, it will create a modulation at the frequency f_{ref} in any φ-sensitive physical measurable, $S(t) = S_0 \cos(2\pi f_{ceo} t + \theta)$. Because the f-to-$2f$ interferometer is used to phase-lock the evolution of φ, the photoelectron emission will itself be phase-locked to the reference signal, $R(t) = R_0 \cos(2\pi f_{ref} t)$. However, as discussed above, there will be a constant, non-vanishing phase offset θ between $R(t)$ and $S(t)$. Using a lock-in detector both the amplitude S_0 and the phase θ of the input signal can be determined. The important feature of the photoelectron emission signal is that the function $\varphi(\theta)$ can be given with sufficient accuracy,

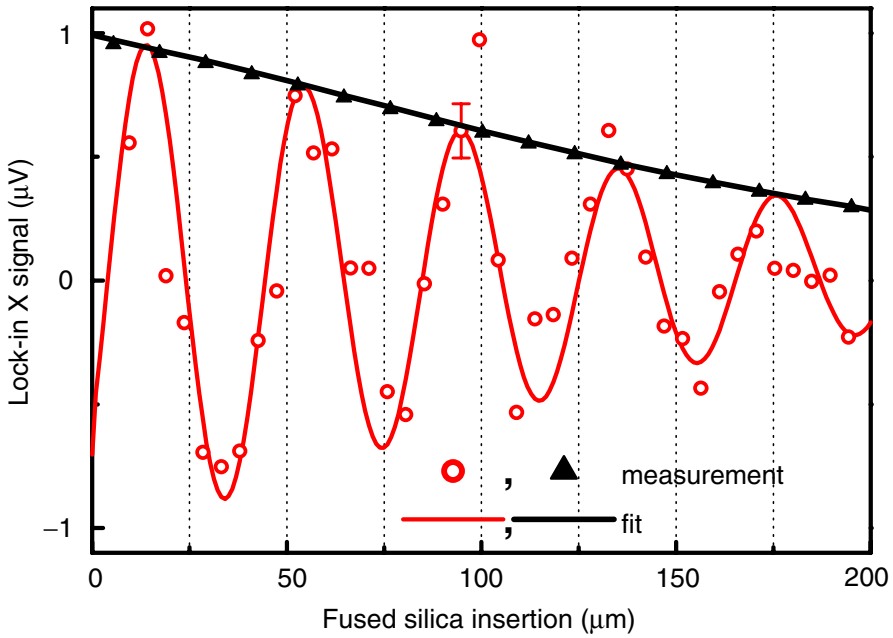

Figure 7. In-phase, $X = S_0 \cos\theta$ component of the lock-in amplifier output as a function of the change in path length through the fused silica glass wedges. The lock-in input is the photoemission signal amplified by the electron multiplier tube. The experimental data (circles) are corrected for a constant (non-oscillating) phase offset of electronic origin. Measuring the glass insertion dependence of the output signal of the electron multiplier tube with the lock-in amplifier referenced to the repetition rate of the laser and the subsequent fit yield the black triangles and the black solid fit. The latter is then used as an envelope function to fit the oscillating lines, giving excellent reproduction of the observed decay in the photoemission signal. The error bar depicts the rms fluctuation of the signal at a fixed ΔL over an acquisition time of 10 min, which is approximately equal to the time taken to collect the data.

unlike the case of the f-to-$2f$ signal coming from the ZnO crystal. For this, the simple relation $\varphi(\theta) = \theta + \varphi_{\max} + 2\pi f_{\mathrm{ref}} t$ is used, where $\varphi_{\max}$ is the CE phase that maximizes the physical measurable $S(t)$. The knowledge of $\varphi_{\max}$ follows from simulations (see section 2). This procedure then implies full information on how the evolution of φ in the pulse train is phased to the reference signal (i.e. at which phase of the reference signal a pulse with, for example, $\varphi = 0$ is interacting with the surface) and thus knowledge of the carrier-envelope phase in any of the emitted laser pulses.

With the servo loop in operation and the lock-in amplifier referenced to f_{ref}, we observed a clearly measurable ac component $S(t)$ of the photoemission signal induced by the phase-controlled 4-fs pulses, as described in [36]. Varying the insertion of the fused silica wedges gave rise to oscillation of the in-phase (X) component of the output of the lock-in amplifier with a periodicity similar to that observed for the f-to-$2f$ signal (red circles in figure 7), indicating that the observed signal originates from a continuous CE phase slippage in the pulse train. The effect was observed only when the sample was moved slightly out of focus, this being attributed to the fact that due to the large angle of incidence applied here different parts of the beam in the focal

vicinity were incident with significantly different Gouy phase shifts exerted on them, which, in general, significantly modifies the phase of any electromagnetic or mechanical wave near the focus [14, 37]. (Note that the Gouy phase is referred to as 'Guoy' in [37].) Thus, detrimental effects are expected to occur due to inherent spatial averaging unless one moves the surface as far off focus as allowed by the signal level. This observation also serves as subsidiary proof that our device was indeed delivering the first experimental verification for the qualitative conclusions of our simulations [36].

Besides the clear oscillation of the $X = S_0 \cos\theta$ component of the lock-in output, its amplitude S_0 also exhibits rapid decay with ΔL as a consequence of dispersive effects, as discussed above. Since we could use the independently determined curve depicted on the same graph as the envelope function, the only fit parameter used for matching the experimental data appears in modelling the shift of θ with ΔL, $\theta = \theta_0 + \pi(\Delta L / L_{\mathrm{pe}})$. The characteristic propagation length causing a π phase shift in the modulation of the photoemission signal was evaluated as $L_{\mathrm{pe}} = 20.3(+2/-1.5)\,\mu\mathrm{m}$ from the fit in figure 7. This value is in good agreement with the computed dephasing length for our 4-fs, 710-nm pulses in fused silica, $L_{\mathrm{deph}} = 22.5\,\mu\mathrm{m}$, specifying the propagation length over which the carrier-envelope phase suffers a π phase shift [2], converting $E_{\mathrm{L}}(t)$ into $-E_{\mathrm{L}}(t)$, assuming an unchanged pulse envelope. Structures in an ultrabroad-band spectrum may cause the dephasing length to deviate appreciably from the approximation formula given in [2]. This applies to our case, where the structured pulse spectrum results in $L_{\mathrm{deph}} = 21.4\,\mu\mathrm{m}$, which is some 5% smaller than predicted by the analytic formula given above for fused silica at $\lambda_0 = 710\,\mathrm{nm}$. This phenomenon will be examined in detail in section 5.

Although the phase dependence of the photocurrent was clearly observable in our experiments, the depth of modulation caused by the slippage of φ is well below 1%, i.e. significantly smaller than predicted by, for example, figure 2 for similar conditions. The origin of this contrast reduction has yet to be more thoroughly investigated, but some potential reasons may be identified.

Surface roughness of the pressed metal cathode coated with gold (as confirmed by atomic force microscopy scans) may reduce the fractional area exposed to a strong $E_{\perp}$ and thereby the phase sensitivity of the overall current emitted. This is because there is not expected to be any CE phase dependence caused by the field vector component that is parallel to the surface (as follows from, for example, the simple picture in section 2). These irregularities can compromise phase measurement in one more way because local field enhancement on them can result in tunnelling photoelectron emission. The CE-phase-dependent modulation of multi-photon-induced emission is phase-shifted by π as compared with the tunnelling regime [25]. This can obviously result in drastic contrast reduction when the surface-integrated emission signal is measured. Surface contamination owing to poor vacuum conditions (10^{-5} mbar) and sample preparation can also reduce CE phase sensitivity. Experiments on ion-induced electron emission [38] (where the Coulomb field strength exerted by the incoming projectile is comparable with the laser field in our experiments) confirmed that agreement between experiment and theory can only be achieved with atomically clean surfaces under ultrahigh vacuum conditions. Forthcoming experiments on crystalline samples kept under higher vacuum will test these hypotheses.

Additionally, mechanical noise of the f-to-$2f$ interferometers, amplitude-to-phase coupling in the fibres used for external spectral broadening [33, 34], etc are all noise sources that—if they appear within the phase-locking servo loop—will be written back onto the output of the laser and will appear as an extra phase noise source in an out-of-loop measurement. This

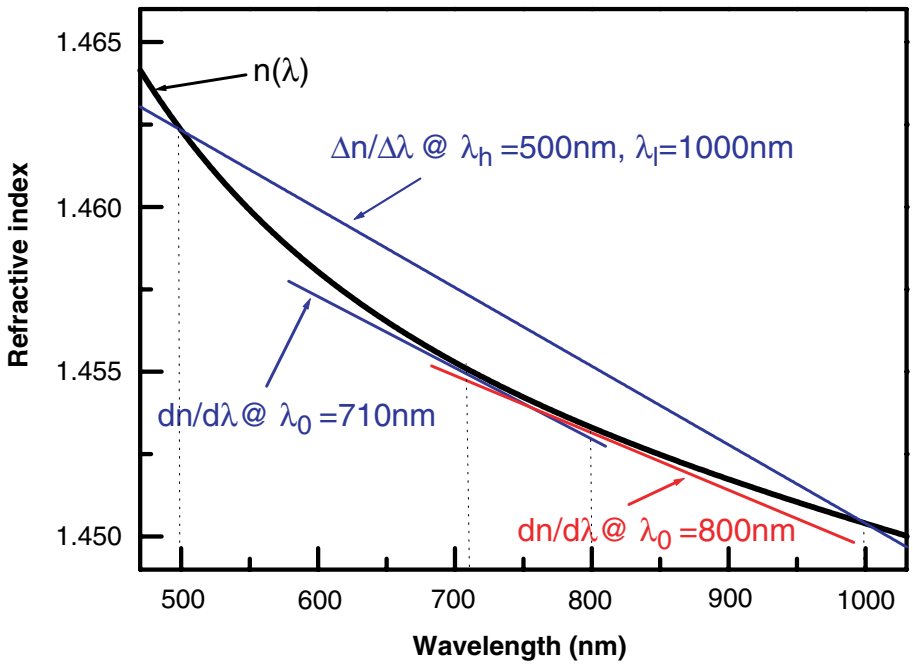

Figure 8. Refractive index of fused silica versus wavelength and the quantities relevant to the phase change of the f-to-$2f$ beat signal and the shift of the carrier-envelope phase with a change in the propagation length through this material. See text for further explanations.

effect, already scrutinized at the end of the previous section, obviously smears the CE phase contrast of the photoemission signal, too. A rough estimation from the measured rms phase noise value (see section 3) yields a contrast reduction of at most 50% in our case. Improving beam pointing stability in the laser system as well as vibration and air flow isolation should thus improve contrast significantly.

5. Comparing the *f*-to-2*f* method and direct phase measurement

Our measurements revealed that both $L_{f\text{-to-}2f}$ and L_{pe} agree, within the experimental accuracy, with the dephasing length, L_{deph}. This would suggest that both the f-to-$2f$ signal and the photoemission signal are, in principle, suitable for measuring φ in the laser pulse train. In general, however, this is not true. In fact, for $L_{f\text{-to-}2f}$, a simple analysis yields $L_{f\text{-to-}2f} = |\Delta n/\Delta\lambda|^{-1}/2$, where $\Delta n/\Delta\lambda = [n(\lambda_{\mathrm{h}}) - n(\lambda_{\mathrm{l}})]/(\lambda_{\mathrm{h}} - \lambda_{\mathrm{l}}) = -[n(\lambda_{\mathrm{h}}) - n(2\lambda_{\mathrm{h}})]/\lambda_{\mathrm{h}}$ and n is the refractive index of the propagation medium. However, for the dephasing length one obtains $L_{\mathrm{deph}} \approx |\mathrm{d}n/\mathrm{d}\lambda|^{-1}/2$, where $\mathrm{d}n/\mathrm{d}\lambda$ is the first derivative of $n(\lambda)$ at the carrier wavelength λ_0 [2]. From these analytic expressions it becomes clear that $L_{f\text{-to-}2f} = L_{\mathrm{deph}}$ holds irrespective of λ_0 if and only if $n(\lambda)$ is a linear function of λ, i.e. in the absence of dispersion. Figure 8 reveals that in a dispersive medium these two quantities (the slope of the respective light and dark blue lines) are only accidentally equal to each other for a specific choice of λ_0 and/or for a special spectral distribution, which happens to apply in our case for λ_0 near 690 nm [26]. By contrast, a carrier wavelength of $\lambda_0 = 800$ nm would imply a dephasing length, L_{deph}, that deviates by

more than 35% from $L_{f\text{-to-}2f}$ at $\lambda_h = 500\,\text{nm}$ in fused silica, i.e. the slope of the red curve in figure 8 appreciably deviates from that of the dark blue.

This has important implications if one intends to stabilize the phase precisely for an extreme non-linear optical experiment carried out with amplified laser beams. Since dispersive path length fluctuations in a complex, multiple-stage amplifier system can easily add up to a value comparable with the dephasing length a phase stabilization system based on the f-to-$2f$ technique will improperly compensate for any phase drift or jitter and perfect on-target phase stabilization will therefore not be achieved. It is thus necessary to carry out direct phase measurement, preferably with a small portion of the beam and preferably using a compact device as demonstrated here. The fact that the f-to-$2f$ technique is unable to measure φ reliably in the presence of dispersion prompts the important question of whether the application of this technique to controlling the evolution of the carrier-envelope phase in a cw mode-locked laser (see [14]–[23]), which always contains dispersive elements, achieves the desired effect, namely control of the carrier-envelope phase evolution. The answer is yes. This is because intracavity dispersion is not permitted to modify the circulating pulse from one round-trip to the next. In the stationary case of cw mode locking, the femtosecond laser pulse precisely reproduces itself in the output pulse train (apart from a possible shift in the carrier-envelope phase) owing to a subtle interplay between non-linear processes and dispersive effects. Because the pulse is always the same except for a shift in its carrier-envelope phase ($\Delta\varphi$), the f-to-$2f$ technique can reliably measure this quantity and stabilize f_{ceo}. In contrast with this, propagation through dispersive elements outside the laser cavity leads to modification of several pulse properties (rather than only φ) simultaneously. Contrary to the difficulties with the f-to-$2f$ technique, L_{pe} is found to be equal to L_{deph} with a good accuracy in our simulations irrespective of the specific choice of the carrier wavelength. This finding backs the simple intuitive arguments presented in section 2.

The validity of the approximation $L_{deph} \approx |dn/d\lambda|^{-1}/2$ is also worth a closer look. We computed the carrier-envelope phase shift of a Gaussian pulse by evaluating propagation equations in a dispersive medium and compared the results given by the approximation formula. The difference between these two quantities is depicted in figure 9 as a function of the propagation distance (in units of the dephasing length in fused silica). For a Gaussian pulse three curves were calculated for pulses having an intensity FWHM duration of 4, 6 and 10 fs. As expected, for a 4-fs pulse the dephasing length approximation breaks down, whereas already a 6-fs Gaussian pulse is 'long enough' (and not so different from a 10-fs-one from this point of view) for its envelope not to change too much during propagation, preserving the validity of the dephasing length approximation.

Apart from the pulse length the actual pulse shape can also influence carrier-envelope phase relations upon propagation. The same calculation was made for the pulse shapes retrieved from measurements with our pulse diagnostic system [26]. Our study reveals that the above approximation fails even more for a pulse with a complex spectral and temporal shape (figure 9). The irregularities observed for the retrieved pulse shape (e.g. the strong deviation in the first part of the curve) are not just limited to its CE phase behaviour since the dependence of the pulse length is just as irregular. These can be explained by the fact that our ultrashort 4-fs pulse with its highly structured spectrum and temporal envelope will suffer significant envelope distortion during propagation in a relatively small amount of dispersive material. After about 70 μm of propagation this difference will stop growing probably owing to the fact that the pulse is now chirped and therefore temporally stretched enough for its envelope not to be affected

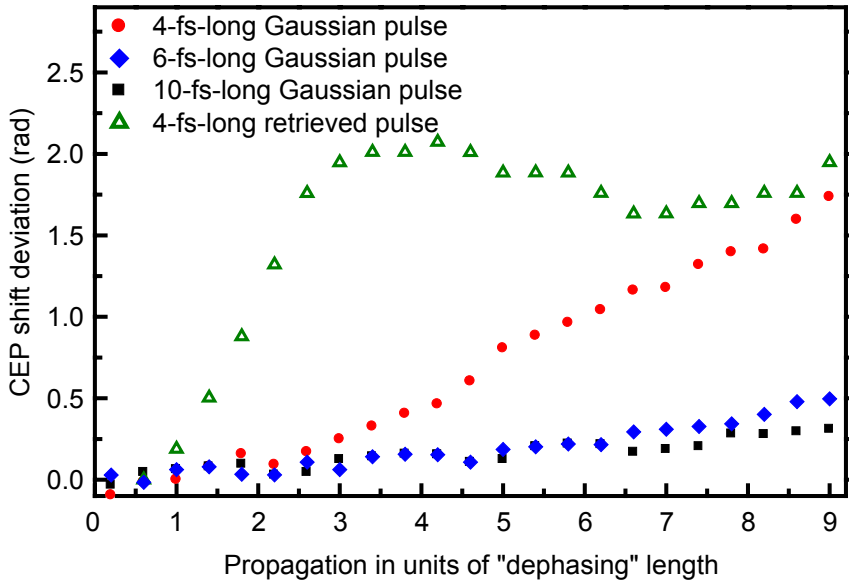

Figure 9. Deviation of the accurate CE phase shift value (taking dispersive pulse distortion into account) from the value calculated according to the dephasing length approximation. Results for pulses with Gaussian envelopes having different pulse lengths are depicted, as well as for a more realistic pulse envelope retrieved from our pulse diagnostic system [26]. The central wavelength is 710 nm in all four cases.

so much by dispersion. In this case, the dephasing length value will provide an acceptable approximation of the CE phase slip, represented by the close-to-horizontal part of the curve.

These simulations back the above conclusion that a direct phase measurement technique is required to stabilize the CE phase against extracavity jitter. Since optical path length fluctuations in a high-power laser system can easily attain the dephasing length, it is of utmost importance to use a method of phase stabilization that is directly sensitive to the relative timing of the electric field oscillation to the pulse envelope peak. Sampling just the spectral wings of the beam, as the f-to-$2f$ technique does, does not provide sufficiently accurate information on the shift of the carrier-envelope phase caused by some change in the optical path length through components outside the phase-stabilized oscillator. This conclusion is also valid for amplified laser systems delivering 5–7 fs pulses typically used for attosecond experiments, since unless one has well-behaved Gaussian pulses the effect of the imperfectness of the f-to-$2f$ phase stabilization will be noticable, as already experimentally observed elsewhere [14].

To overcome these limitations a compact, single-shot version of the above-described solid-state-based phase detector can be proposed containing just two electrodes sealed in a glass bulb with a thin input window. From such a device using 5–7 fs, 10 μJ pulses (a small portion split off from a typical amplifier/compressor output) one can expect considerable multi-photon-induced photoelectron emission signals that could be measured directly (without the multiplier tube). After calibration and correcting for the pulse-to-pulse energy jitter that can be measured independently and synchronously with a photodiode the phase evolution can be assessed practically real-time in the typically 1-kHz-amplified pulse train. Corresponding correction can then be applied to achieve exact on-target phase stabilization.

6. Summary

We have shown that multi-photon-induced photoelectron emission directly probes the carrier-envelope phase and allows determination of the actual value of φ of any pulse delivered by a phase-controlled, mode-locked laser system. According to our analysis, the maximum photocurrent indicates the arrival of a pulse with $\varphi \approx -\pi/4$. This phase calibration value is robust against pulse shape and intensity fluctuations in the multi-photon-induced emission regime. This technique, combined with standard pulse (envelope) diagnostic systems, is capable of precisely measuring and controlling the electric (as well as magnetic) field evolution of an ultrashort laser pulses since it can measure the carrier-envelope phase directly, unlike the widely used f-to-$2f$ interferometric technique. This feature is of great importance in extreme non-linear optical experiments in which direct phase measurement is needed to stabilize the phase precisely and on the target. Our device has the advantages of being compact, being operational at a fraction of typical energy levels of amplified laser systems and of having the potential of single-shot operation. It opens the door to controlling and probing condensed matter dynamics within the wave cycle of visible light, i.e. on a sub-femtosecond time scale.

Acknowledgments

We gratefully acknowledge the contributions of G Tempea, V Yakovlev, T Fuji and A Unterhuber to setting up and characterizing the 4-fs laser system. We also thank G Farkas, C Tóth, A Baltuška, A Scrinzi, G Steinmeyer, and M Ivanov for illuminating discussions. We are indebted to the Department of Physics, University of Bath for supply of the photonic crystal fibre. M Kakehata and K Torizuka acknowledge the financial support by the Budget for Nuclear Research of the Japanese Ministry of Education, Culture, Sports, Science and Technology, based on the screening and counselling by the Atomic Energy Commission. The work was sponsored by the FWF (Austria, grants F016, P15382 and Z63) and by the European ATTO network.

References

[1] Xu L, Spielmann Ch, Poppe A, Brabec T, Krausz F and Hänsch T W 1996 *Opt. Lett.* **21** 2008
[2] Brabec T and Krausz F 2000 *Rev. Mod. Phys.* **72** 545
[3] Cormier E and Lambropoulos P 1998 *Eur. Phys. J.* D **2** 15
[4] Christov I P 2000 *Appl. Phys.* B **70** 459
[5] Dietrich P, Krausz F and Corkum P B 2000 *Opt. Lett.* **25** 16
[6] Mehendale M, Mitchell S A, Likforman J-P, Villeneuve D M and Corkum P B 2000 *Opt. Lett.* **25** 1672
[7] Yudin G L and Yu Ivanov M 2001 *Phys. Rev.* A **64** 013409
[8] Chelkowski S and Bandrauk A D 2002 *Phys. Rev.* A **65** 061802
[9] Kakehata M, Kobayashi Y, Takada H and Torizuka K 2002 *Opt. Lett.* **27** 1247
[10] Mücke O D, Tritschler T, Wegener M, Morgner U and Kärtner F X 2002 *Opt. Lett.* **27** 2127
[11] Milosevic D B, Paulus G G and Becker W 2002 *Phys. Rev. Lett.* **89** 153001
[12] Roos P A, Quraishi Q, Cundiff S T, Bhat R D R and Sipe J E 2003 *Opt. Express* **11** 2081
[13] Paulus G G, Grasbon F, Walther H, Villoresi P, Nisoli M, Stagira S, Priori E and De Silvestri S 2001 *Nature* **414** 182
[14] Paulus G G, Lindner F, Walther H, Baltuška A, Goulielmakis E, Lezius M and Krausz F 2003 *Phys. Rev. Lett.* **91** 253004
[15] Baltuška A *et al* 2003 *Nature* **421** 611

[16] Reichert J, Holzwarth R, Udem Th and Hänsch T W 1999 *Opt. Commun.* **172** 59
[17] Telle H R, Steinmeyer G, Dunlop A E, Stenger J, Sutter D H and Keller U 1999 *Appl. Phys.* B **69** 327
[18] Kakehata M, Takada H, Kobayashi Y, Torizuka K, Fujihira Y, Homma T and Takahashi H 2001 *Opt. Lett.* **26** 1436
[19] Jones D J, Diddams S A, Ranka J K, Stentz A, Windeler R S, Hall J L and Cundiff S T 2000 *Science* **288** 635
[20] Apolonski A, Poppe A, Tempea G, Spielmann Ch, Udem Th, Holzwarth R, Hänsch T W and Krausz F 2000 *Phys. Rev. Lett.* **85** 740
[21] Holzwarth R, Udem Th, Hänsch T W, Knight J C, Wadsworth W J and Russell P St J 2000 *Phys. Rev. Lett.* **85** 2264
[22] Morgner U, Ell R, Metzler G, Schibli T R, Kärtner F X, Fujimoto J G, Haus H A and Ippen E P 2001 *Phys. Rev. Lett.* **86** 5462
[23] Helbing F W, Steinmeyer G, Keller U, Windeler R S, Stenger J and Telle H R 2002 *Opt. Lett.* **27** 194
[24] Udem Th, Holzwarth R and Hänsch T W 2002 *Nature* **416** 233
[25] Lemell Ch, Tong X-M, Krausz F and Burgdörfer J 2003 *Phys. Rev. Lett.* **90** 076403-1
[26] Yakovlev V, Dombi P, Tempea G, Lemell Ch, Burgdörfer J, Udem Th and Apolonski A 2003 *Appl. Phys.* B **76** 329
[27] Schenkel B, Biegert J, Keller U, Vozzi C, Nisoli M, Sansone G, Stagira S, De Silvestri S and Svelto O 2003 *Opt. Lett.* **28** 1987
[28] Yamane K, Zhang Z, Oka K, Morita R, Yamashita M and Suguro A 2003 *Opt. Lett.* **28** 2258
[29] Helbing F W, Steinmeyer G and Keller U 2003 *Laser Phys.* **4** 644
Steinmeyer G 2003 private communication
[30] Tempea G, Yakovlev V, Bacovic B, Krausz F and Ferencz K 2001 *J. Opt. Soc. Am.* B **18** 1747
[31] Fortier T M, Jones D J, Ye J, Cundiff S T and Windeler R S 2002 *Opt. Lett.* **27** 1436
[32] Witte S, Zinkstok R T, Hogervorst W and Eikema K S E 2004 *Appl. Phys.* B **78** 5
[33] Fortier T M, Ye J, Cundiff S T and Windeler R S 2002 *Opt. Lett.* **27** 445
[34] Ames J N, Ghosh S, Windeler R S, Gaeta A L and Cundiff S T 2003 *Appl. Phys.* B **77** 279
[35] Tóth Cs, Farkas Gy and Vodopyanov K L 1991 *Appl. Phys.* B **53** 221
[36] Apolonski A *et al* 2004 *Phys. Rev. Lett.* **92** 073902
[37] Siegman A E 1986 *Lasers* (Mill Valley, CA: University Science Books) ch 17.4
[38] Winter H 2002 *Phys. Rep.* **367** 387